CCS Chemistry

RESEARCH ARTICLE

Received: Sept. 29, 2021 | Accepted: Jan. 25, 2022 | Published: Feb. 24, 2022

Multiple Resonance Thermally Activated Delayed Fluorescence Sensitizers Enable Green-to-Ultraviolet Photon Upconversion: Application in Photochemical Transformations

Yaxiong Wei[1,2], Ke Pan[1], Xiaosong Cao[1]*, Yuanming Li[3], Xiaoguo Zhou[3] & Chuluo Yang[1]*

[1]*Shenzhen Key Laboratory of Polymer Science and Technology, College of Materials Science and Engineering, Shenzhen University, Shenzhen 518060,* [2]*School of Physics and Electronic Information, Anhui Normal University, Wuhu, Anhui 241000,* [3]*Department of Chemical Physics, University of Science and Technology of China, Hefei, Anhui 230026*

**Corresponding authors: xcao@szu.edu.cn; clyang@szu.edu.cn*

Cite this: *CCS Chem.* **2022**, 4, 3852–3863
DOI: 10.31635/ccschem.022.202101507

Efficient visible-to-ultraviolet (UV) triplet–triplet annihilation upconversion (TTA-UC) with large anti-Stokes shift is highly promising for solar-powered and indoor applications. Nonetheless, the excitation wavelength is confined to the blue region (<450 nm), mainly due to large energy loss during triplet sensitization, resulting in reduced photon utilization efficiency in practical scenarios. Herein, a series of multiple resonance thermally activated delayed fluorescence (MR-TADF) compounds are developed as purely organic sensitizers for the purpose of energy-loss reduction, which also feature intense absorbance in the visible region, high intersystem crossing efficiencies, and long triplet lifetimes. By pairing the MR-TADF sensitizers with appropriate acceptors, green-to-UV TTA-UC systems were realized with an anti-Stokes shift up to 1.05 eV, upconversion quantum yield up to 8.6%, and threshold excitation intensity as low as 9.2 mW cm^{-2} in solution. The TTA-UC pairs were applied as internal or external sources of UV photons to trigger energy-demanding photopolymerization and photoligation reactions even under excitation of low-power-density green light-emitting diode light, revealing the broad utility of these molecular upconverters. This work unlocks the huge potential of MR-TADF-type sensitizers in upconversion applications.

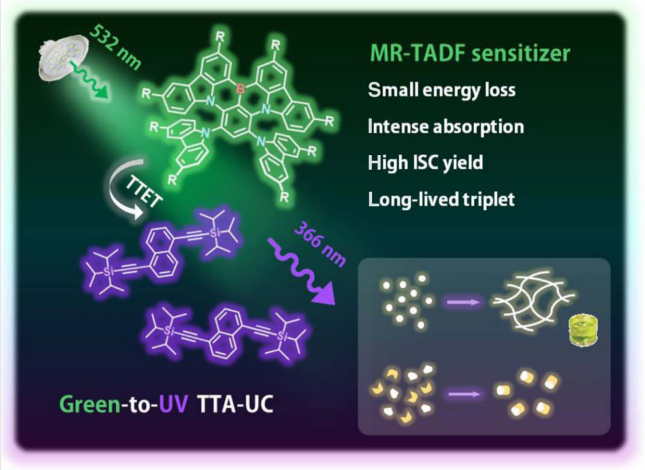

Keywords: triplet–triplet annihilation upconversion, visible-to-ultraviolet upconversion, multiple resonance, photochemical reactions

Introduction

Triplet–triplet annihilation upconversion (TTA-UC), or triplet fusion, is an anti-Stokes shifting technique that converts low-energy incident light under weak irradiation intensity to high-energy photons.[1,2] Compared to other photon upconversion methods, including two-photon absorption and rare-earth upconversion, TTA-UC enjoys a low power density requirement and a high upconversion quantum yield (Φ_{UC})[3] and has attracted considerable attention in photovoltaics,[4,5] photocatalysis,[6-8] bioimaging,[9,10] organic light-emitting diodes (OLEDs),[11] circularly polarized luminescence,[12] and photoinduced drug release.[13] By pairwise selection of sensitizers and acceptors, the applicability of the TTA-UC system featuring adjustable excitation/emission wavelengths has been demonstrated.[14,15] Notably, visible-to-ultraviolet (UV) upconversion is particularly valuable for enhancing the efficiency of photochemical systems, including H_2 generation, CO_2 reduction, and many organic transformations[16,17] that always require a highly energetic excited state to induce challenging bond activation/formation reactions.[18]

Implementation of visible-to-UV TTA-UC with a concurrent large anti-Stokes emission shift, high Φ_{UC}, and a low power density threshold (I_{th}) is essential for solar-powered and indoor applications but remains elusive.[19] It is important to note that among all reported visible-to-UV TTA-UC systems, the energy gains are <0.92 eV, restricting the excitation wavelengths to the violet or blue regions (Scheme 1c and Supporting Information Figure S1 and Table S1). This limitation is mainly caused by the inherent energy loss during $S_1^*\rightarrow S_1$ vibrational relaxation (VR) and the intersystem crossing (ISC) process of the sensitizers.[20,21] As illustrated in the Jablonski diagram in Scheme 1a, the sum of the reorganization energy (λ_S^*) and the gap between singlet and triplet excited states (ΔE_{ST}) is always >0.5 eV.[19,22] To minimize energy loss for triplet sensitization, there have been recent advances by using direct S_0-T_1 absorption sensitizers, but low triplet energy (<1.8 eV) and the short triplet lifetime (~10^2 ns) of these complexes circumvent their use in visible-to-UV TTA-UC.[23-25] A more practical route is to adopt donor–acceptor (D–A) typed thermally activated delayed fluorescence (TADF) molecules owing to their energy degeneracy between excited states (ΔE_{ST} < 100 meV), which also allows efficient ISC courses from $S_1\rightarrow T_1$ in the absence of noble metals.[26] For instance, several groups have independently reported the use of carbazolyl dicyanobenzene-based TADF molecules to sensitize *p*-terophenyl or pyrene derivatives, and achieved anti-Stokes shifts up to 0.83 eV under photoirradiation below 450 nm.[27-29] Nonetheless, the large structural flexibility of the charge-transfer-featured S_1 state would result in substantial non-radiative

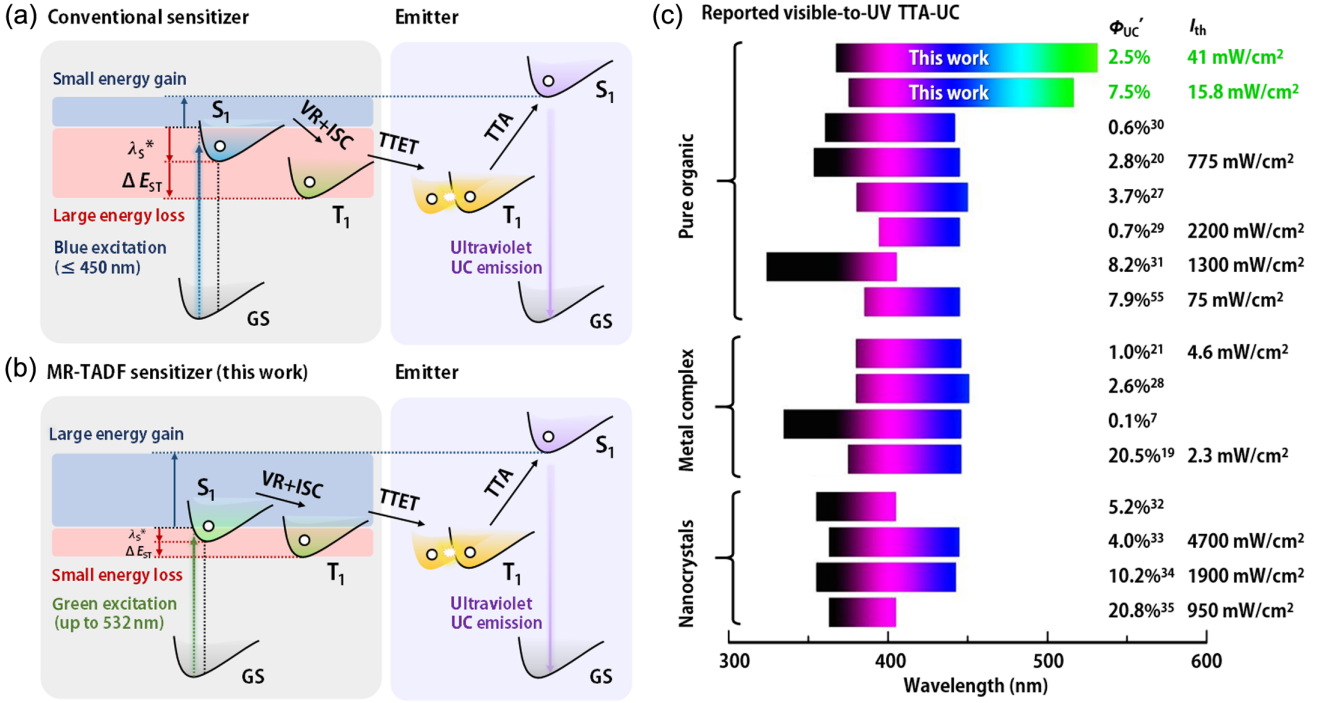

Scheme 1 | *Mechanism of visible-to-UV photon upconversion employing (a) conventional sensitizer with large energy loss and (b) MR-TADF sensitizer with small energy loss during $S_1^*\rightarrow S_1$ VR and $S_1\rightarrow T_1$ ISC process. λ_S^* is the reorganization energy, ΔE_{ST} is the gap between singlet and triplet excited states. (c) Summary of reported visible-to-UV TTA-UC by using different types of sensitizers.*[7,19-21,27-35,55]

DOI: 10.31635/ccschem.022.202101507
Citation: *CCS Chem.* **2022**, 4, 3852–3863
Link to VoR: https://doi.org/10.31635/ccschem.022.202101507

energy loss and cause weak absorption in the visible range, leading to high excitation threshold that was not even close to solar irradiance.[20]

In this context, new sensitizers with satisfactory molar extinction coefficients (ε) and absorption beyond the blue region (i.e., >500 nm) while maintaining high triplet energies (i.e., >2.2 eV), high ISC efficiency (Φ_{ISC}), and long triplet lifetimes becomes an emergent request. It is also noteworthy that the development of metal-free triplet sensitizers is an ongoing pursuit, considering the toxicity and poor energy-level tunability of precious- or rare-earth-metal-based complexes.[36,37] In light of these stringent demands, we hereby report for the first time a highly efficient green-to-UV TTA-UC system operable with weak incident light by implementing multiresonance TADF (MR-TADF) compounds as photosensitizing species. The MR effect induced by the *ortho*-positioned, electron-rich N-atom and the electron-deficient B-atom in a rigid polycyclic aromatic hydrocarbon framework minimizes the VR of S_1, and separates frontier molecular orbitals to ensure small ΔE_{ST}.[38–40] Additionally, these compounds typically display a much more intense absorption band caused by short-range charge-transfer, which is a significant advantage compared to the D–A typed counterparts (Supporting Information Scheme S1).[41] These features render MR-TADF compounds superior candidates as triplet donor with increased sensitivity for weak incident light and broader choice of acceptors (Scheme 1b). To maximize the anti-Stokes shift, energy loss during triplet–triplet energy transfer (TTET) is further reduced by matching the MR-TADF sensitizers with the appropriate acceptors to give small or even negative triplet energy gaps, eventually leading to an unprecedentedly large energy gain of 1.05 eV among visible-to-UV TTA-UC materials. Ensured by the efficient UV-photon generation under weak excitation intensity, these systems can be successfully utilized to trigger energy-demanding photochemical reactions with low-power green light.

Experimental Methods

Instruments and general methods

^{1}H NMR spectra were recorded with a Bruker AVANCE III 500 superconducting-magnet high-field NMR spectrometer (Bruker, Switzerland) at 500 MHz, where $CDCl_3$ or CD_2Cl_2 was used as solvent and tetramethylsilane was the standard for which δ = 0.00 ppm. High-resolution mass spectra were measured using an Agilent 7250 (Agilent, United States) and JEOL-JMS-T100LP AccuTOF (JEOL, Japan). UV–vis absorption spectra were recorded with a Shimadzu UV-2700 spectrophotometer (Shimadzu, Japan) at 25 °C. Steady-state photoluminescence (PL) spectra were measured with a fluorescence spectrophotometer (F-7100, Hitachi, Japan). The transient PL decay curves were obtained by FluoTime 300 (PicoQuant GmbH, Germany) with a Picosecond Pulsed LASTER (LASTER480) as the excitation source. The fluorescence quantum yields were measured on a Hamamatsu UV-NIR absolute PL quantum yield spectrometer (C13534, Hamamatsu Photonics, Japan) equipped with a calibrated integrating sphere, and the integrating sphere was purged with dry argon to maintain an inert atmosphere. The general procedure for the synthesis of sensitizers and acceptors, calculation methods of TTA-UC quantum yields, and TTET efficiency are listed in the Supporting Information.

TTA-UC spectra

TTA-UC spectra were recorded using a homemade fluorescence emission spectrometer. A semiconductor laser (517 or 532 nm) was selected as the excitation light source. The diameter of the laser spot was ~5 mm. In the TTA upconversion experiments, the solutions mixing sensitizer and acceptor were prepared in a glove box and kept in a quartz cuvette (10 mm × 1 mm). In experiments, the upconverted fluorescence of acceptors was collected and detected with a commercial fiber-optic spectrometer (ULS2048-2-USB2, AvaSpec, Avantes, Netherlands), under photoexcitation at 517 nm (or 532 nm).

Computational methods

Geometries of the compounds were optimized using density functional theory (DFT) with the B3LYP function and 6-31G(d) basis set. The spin-density surfaces of the compounds and the energy gaps between ground state and lowest triplet state were calculated with the time-dependent DFT (TD-DFT) level using the same basis set. The vertical excitation energies were directly compared with absorption spectra, and the corresponding electronic transitions were identified subsequently. The polarized continuum model (PCM) model was applied to evaluate the solvent effect. All these calculations were performed with the Gaussian 09W program package.

The spin-orbital couplings (SOCs) between S_1 and T_n (n = 1, 2, 3) states were calculated with PySOC by considering that the three T_n substrates (m = 1, 0, –1) are degenerate, that is, $\langle S_1|\hat{H}_{SOC}|T_1\rangle = \sqrt{\Sigma_{m=0,\pm1}\langle S_1|\hat{H}_{SOC}|T_1{}^m\rangle^2}$, where $\hat{H}_{soc}$ represents the interaction of the SOC. All SOCs were obtained at the TD-DFT level of theory using the B3LYP functional and the 6-31G(d) basis set.

Results and Discussion

The advent of MR-TADF molecules has brought exciting opportunities for the fabrication of OLEDs with extraordinary efficiency and color purity,[26,42] yet their potential as sensitizers remains underexplored. An important issue to be addressed is the insufficient Φ_{ISC} of MR-TADF compounds compared to conventional (D–A typed) TADF

DOI: 10.31635/ccschem.022.202101507
Citation: *CCS Chem.* **2022**, 4, 3852–3863
Link to VoR: https://doi.org/10.31635/ccschem.022.202101507

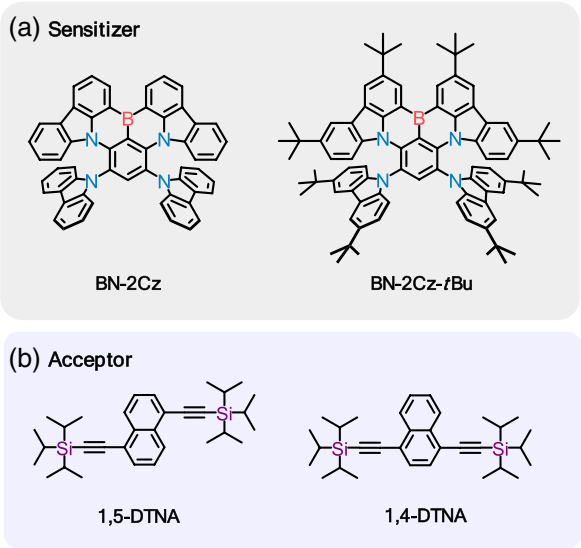

Scheme 2 | *Molecular structures of (a) the MR-TADF sensitizers and (b) ethynyl naphthalene-based acceptors.*

fluorophore, as also reflected by the smaller contribution of long-lived delayed components of the photoluminescence quantum yields (Φ_{PL}s).[43] This characterization is related to the pseudo spin-forbidden nature of the $S_1 \rightarrow T_1$ transition with slightly enlarged energy differences (typically in the range of 100–200 meV).[41] To overcome this obstacle, we established two MR-TADF compounds (BN-2Cz and BN-2Cz-*t*Bu, Scheme 2a) with twisted geometry as highly promising heavy-element-free sensitizers (Supporting Information Schemes S2 and S3 and Figures S2–S12, see Supporting Information for detailed synthetic procedures and characterizations). Importantly, the electronic donors (carbazole or 3,6-di-*tert*-butylcarbazole) orthogonally linked to the parent *B*,*N*-skeleton not only shifted the absorbance into the green region but also guaranteed high Φ_{ISC}.

Characterization of MR-TADF sensitizers and acceptors

The UV–vis absorption spectra, fluorescence, and phosphorescence (recorded at 77 K) emission spectra were measured and are shown in Figure 1. BN-2Cz displayed a strong absorption band at 490 nm ($\varepsilon = 2.37 \times 10^5$ M^{-1} cm^{-1}) in toluene, attributable to the multiple resonance charge transfer transition (Figure 1a). The intense mirroring fluorescence emission was located at 522 nm (Φ_{PL} = 70%), followed by the phosphorescence emission peaking at 554 nm (2.24 eV). Attaching *tert*-butyl (*t*-Bu) moieties to the 3,6-position of the carbazole unit decreased the delocalization energy of electronic states and led to a moderate bathochromic shift of the absorption peak (504 nm, $\varepsilon = 2.95 \times 10^5$ M^{-1} cm^{-1}). Meanwhile, the fluorescence and phosphorescence emission peaks were also shifted to 543

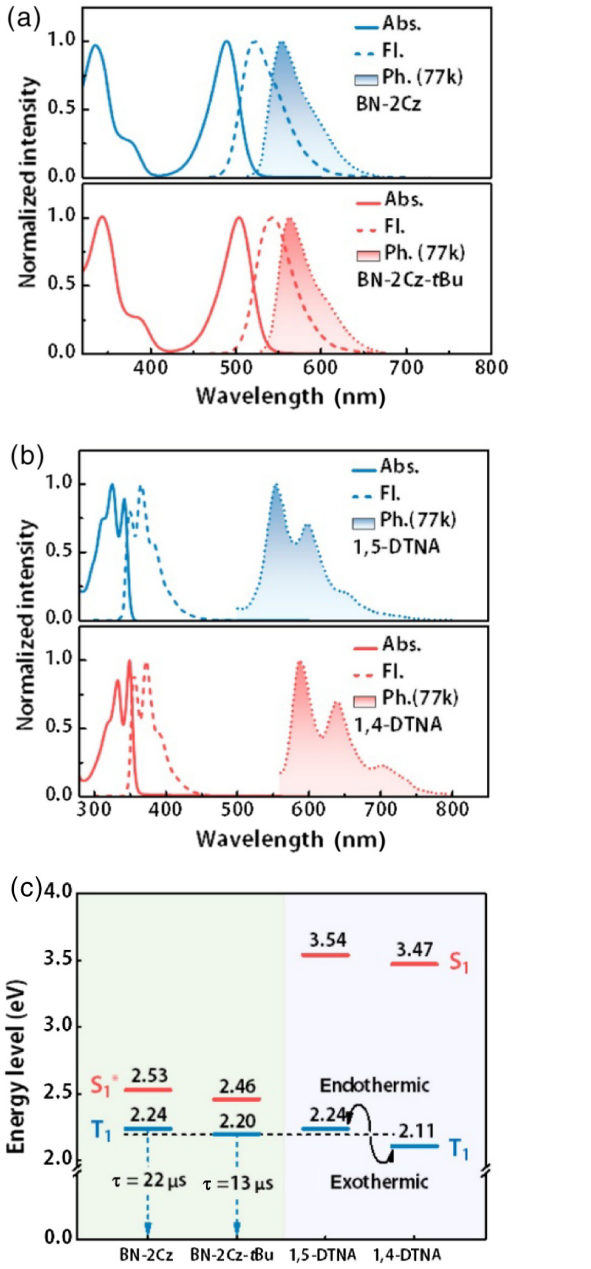

Figure 1 | *Normalized UV–vis absorption (Abs.), fluorescence emission (Fl.), and phosphorescence (Ph.) spectra of (a) sensitizers and (b) acceptors in toluene (c = 0.01 mM). (c) Singlet and triplet energy levels of sensitizers and acceptors, estimates based on (a) and (b).*

and 569 nm (2.20 eV), respectively, with Φ_{PL} as high as 84%. Accordingly, the total energy losses were estimated to be only 0.29 and 0.26 eV during triplet sensitization for BN-2Cz and BN-2Cz-*t*Bu (Figure 1c), respectively. These results also demonstrated that delicate manipulation of excited state energy levels are possible via structural modification.[26]

Time-resolved PL measurements (λ_{ex} = 480 nm) unveiled distinct double-exponential decay profiles for both

DOI: 10.31635/ccschem.022.202101507
Citation: *CCS Chem.* **2022**, 4, 3852–3863
Link to VoR: https://doi.org/10.31635/ccschem.022.202101507

Table 1 | *Photophysical Parameters of Sensitizers and Acceptors*

Compound	λ_{abs}[a]	λ_{fl}[b]	λ_{ph}[c]	Φ_{PL}[d]	Φ_{ISC}[e]	k_{TTET}[f]	Φ_{UC}'[g]
BN-2Cz	490 (2.37)	522	554	70	75	1.34 (0.95)	8.6 (6.9)
BN-2Cz-*t*Bu	504 (2.95)	543	563	84	60	0.25 (0.08)	3.7 (3.4)
1,5-DTNA	326 (1.95); 343 (1.74)	350/366	554/599	73	–	–	–
1,4-DTNA	333 (2.85); 350 (3.34)	357/373	588/638	81	–	–	–

[a] Maximum absorption peaks, nm (molar extinction coefficient, 10^5 M^{-1} cm^{-1}).
[b] Fluorescence emission peaks, nm.
[c] Phosphorescence emission peaks, nm.
[d] Absolute fluorescence quantum yield in Ar, %, measured with excitation wavelength at 475 nm (BN-2Cz), 480 nm (BN-2Cz-*t*Bu), 327 nm (1,5-DTNA), and 333 nm (1,4-DTNA).
[e] ISC efficiency, %.
[f] Bimolecular quenching rate constant with 1,4-DTNA as acceptor (1,5-DTNA as acceptor), 10^9 M^{-1} s^{-1}.
[g] Φ_{UC}' values with 1,4-DTNA as acceptor (1,5-DTNA as acceptor), %, *c*[sensitizer] = 0.01 mM, λ_{ex} = 517 nm.

compounds in deoxygenated toluene solution, characteristic of TADF properties. The prompt fluorescence lifetimes (τ_ps) and delayed lifetimes (τ_ds) were determined to be 4.5 ns (24.9%) and 21.8 μs (75.1%) for BN-2Cz, 5.2 ns (40.5%) and 17.8 μs (59.5%) for BN-2Cz-*t*Bu, respectively (Supporting Information Figures S13 and S14). The long-lived components for both compounds were strongly quenched in air-saturated solution, indicating the origination of delayed fluorescence from triplet states. Based on the Φ_{PL} values and transient PL decay characteristics, the ISC rates (k_{ISC}s) and Φ_{ISC}s were deduced to be 1.1×10^8 s^{-1} and 60% for BN-2Cz-*t*Bu, 1.7×10^8 s^{-1} and 75% for BN-2Cz (detailed calculation in Supporting Information Table S2), respectively, suggestive of an efficient ISC process for triplet sensitization (Table 1). In stark contrast, the parent molecule BN (BN-2Cz-*t*Bu without orthogonally linked substituents) exhibited similar ΔE_{ST} (0.15 eV) value but a feeble delayed fluorescence signal, reflective of weak ISC (Supporting Information Figure S15). To uncover the inherent factors that govern these excited-state properties, we carried out TD-DFT calculations and predicted the SOC matrix elements (ξ) between excited states for BN-2Cz-*t*Bu ($\xi_{S1\text{-}T1}$ = 0.112 cm^{-1}, $\xi_{S1\text{-}T2}$ = 0.653 cm^{-1}), BN-2Cz ($\xi_{S1\text{-}T1}$ = 0.116 cm^{-1}, $\xi_{S1\text{-}T2}$ = 0.802 cm^{-1}, Supporting Information Table S3) and BN ($\xi_{S1\text{-}T1}$ = 0.054 cm^{-1}, $\xi_{S1\text{-}T2}$ = 0.131 cm^{-1}). Since $\Delta E_{S1\text{-}T2}$s were small enough in all cases (<0.16 eV, Supporting Information Table S4), these results hinted at the transition between S_1/T_2 could be a more efficient ISC pathway compared to S_1/T_1 with nearly identical orbital parentages, in line with El-Sayed rules.[44–46] Importantly, the introduction of auxiliary donating groups to form a twisted D–A geometry was the key to induce a much larger orbital difference between S_1 and T_2 in BN-2Cz-*t*Bu and BN-2Cz (Supporting Information Figures S16 and S17),[47] which consequentially facilitated the spin-flip transition and made them more suitable sensitizer candidates.

The tiny Stokes shifts and high triplet energy levels (2.20–2.24 eV) of BN-2Cz and BN-2Cz-*t*Bu allowed them to pair with UV-emissive triplet acceptors. Referring to a recent report by Yanai et al.,[19] we expected that 1,4-bis((triisopropylsilyl)ethynyl)naphthalene (1,4-DTNA, Scheme 2b) would be a suitable acceptor due to its appropriate triplet energy (T_1 = 2.11 eV) and high statistical probability to generate the singlet excited state (*f* = 32%). It was also anticipated that chemical structure modification of ethynyl naphthalene derivatives would allow simultaneous manipulation of both singlet and triplet excited states, thus minimizing enthalpic energy loss in TTET and maximizing the anti-Stokes shift value. Based on computational results for a series of isomers (Supporting Information Figure S18), a new acceptor 1,5-bis((triisopropylsilyl)ethynyl)naphthalene (1,5-DTNA) was also constructed with a smaller π-conjugated structure and slightly higher triplet energy. Correspondingly, toluene solution of 1,5-DTNA (0.01 mM) displayed a hypsochromic shifted 0–0 absorption peak at 343 nm ($\varepsilon = 1.74 \times 10^5$ M^{-1} cm^{-1}) compared to that of 1,4-DTNA (350 nm, $\varepsilon = 3.34 \times 10^5$ M^{-1} cm^{-1}) (Figure 1b and Table 1). Following a similar trend, the 0–0 vibronic fluorescence and phosphorescence peaks were located at 350 nm, 554 nm (2.24 eV) for 1,5-DTNA, and 357 nm, 588 nm (2.11 eV) for 1,4-DTNA. The Φ_{PL} of 1,5-DTNA (73.3% in Ar) was only slightly lower than that of 1,4-DTNA (80.5% in Ar). Based on the energy relationships (Figure 1c), the sensitizer/acceptor pairs were separated into two categories: BN-2Cz/1,4-DTNA, BN-2Cz/1,5-DTNA, and BN-2Cz-*t*Bu/1,4-DTNA as exothermic/isoenergetic systems, and BN-2Cz-*t*Bu/1,5-DTNA as endothermic systems. Though the energy transfer process in the latter combination was thermodynamically unfavorable, the energy barrier was still sufficiently small (0.04 eV) to allow thermally activated TTET.[48] According to earlier reports,[48] the long triplet lifetime of the sensitizer was also beneficial to suppress the deleterious reverse triplet energy transfer (RTET) process, which is a primary cause of low efficiency in endothermic systems. It is hence expected that pairing a sensitizer and acceptor

DOI: 10.31635/ccschem.022.202101507
Citation: *CCS Chem.* **2022**, 4, 3852–3863
Link to VoR: https://doi.org/10.31635/ccschem.022.202101507

with a negative energy difference (ΔE_T) would be viable in our study to enlarge energy gain without significantly deteriorating the TTA-UC performance.

TTET process between sensitizers and acceptors

The TTET process was subsequently investigated between sensitizers and acceptors (Figure 2a and Supporting Information Figure S20). For instance, the delayed fluorescence was gradually quenched upon titration of the BN-2Cz solution with 1,4-DTNA, indicating the occurrence of effective TTET from the sensitizer to the acceptor (Figure 2a). The observed bimolecular quenching rate constant (k_{TTET}) values derived from the Stern–Volmer plots (Figure 2b) were determined to be 1.34 × 10^9 M^{-1} s^{-1} for BN-2Cz/1,4-DTNA and 0.95 × 10^9 M^{-1} s^{-1} for BN-2Cz/1,5-DTNA, and allowed the use of relatively low concentration of acceptors (*c*[sensitizer] = 0.01 mM, *c*[acceptor] = 1 mM) to reach satisfactory TTET efficiency (Φ_{TTET}s > 95%, Supporting Information Table S5). By replacing the sensitizer with BN-2Cz-*t*Bu, the collision energy transfer process was mitigated according to drastically lowered k_{TTET} of 0.25 × 10^9 M^{-1} s^{-1} for BN-2Cz-*t*Bu/1,4-DTNA. This phenomenon was associated with the shielded spin-density surface of T_1 by the insulating *t*-Bu groups that clearly lowered the Dexter electron exchange probability between energy transfer pairs (Supporting Information Figure S19).[49] Due to its endothermic nature, BN-2Cz-*t*Bu/1,5-DTNA presented even smaller k_{TTET} of 0.08 × 10^9 M^{-1} s^{-1}. To compensate the retarded TTET when using BN-2Cz-*t*Bu as the sensitizer, we optimized [acceptor] to 5 mM in the following TTA-UC measurements to attain the relatively high Φ_{TTET}s value of 94% for BN-2Cz-*t*Bu/1,4-DTNA and 82% for BN-2Cz-*t*Bu/1,5-DTNA (Supporting Information Table S6). Notably, increasing [acceptor] is also vital for suppressing the notorious RTET process and providing an entropic driving force in endothermic systems. For BN-2Cz-*t*Bu/1,5-DTNA (ΔE_T = −0.04 eV) specifically, the effect of RTET on TTA-UC performance could be neglected with optimized [acceptor] based on the following relationship: k_{RTET} × [sensitizer] = 0.32 × 10^4 s^{-1} << k_{TTET} × [acceptor] = 0.35 × 10^6 s^{-1}, where the k_{RTET} was estimated to be 0.32 × 10^9 M^{-1} s^{-1} from the equation $k_{RTET} = k_{TTET} \times \exp(\Delta E_T / k_B T)$.[50]

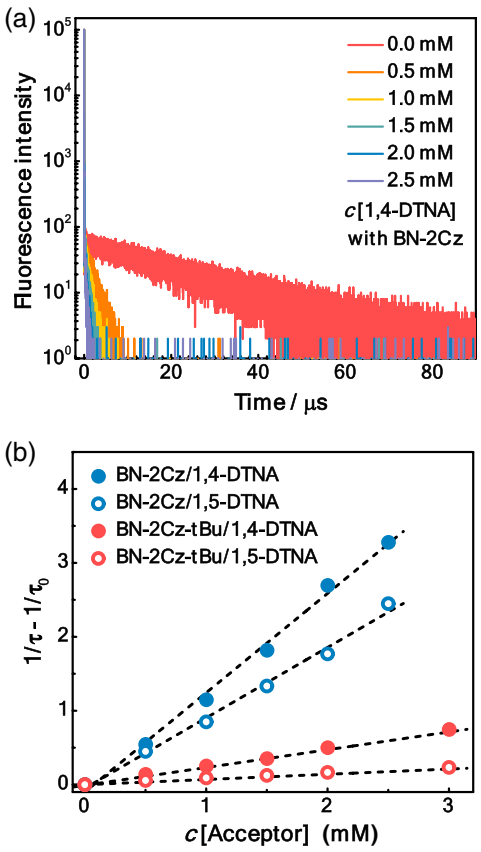

Figure 2 | *(a) Variation of delayed fluorescence lifetime of BN-2Cz with different concentrations of the acceptor 1,4-DTNA. (b) The bimolecular quenching rate generated from the delayed fluorescence lifetime quenching curves. Toluene as the solvent, c[sensitizer] = 0.01 mM, λ_{ex} = 480 nm.*

TTA-UC property in solution

TTA-UC investigations employing the MR-TADF sensitizers and ethynyl naphthalene-based acceptors were subsequently conducted under 517 nm photoexcitation. Intense fluorescence in the range of 330–440 nm that overlapped with the emission of the acceptors could be detected in a deaerated toluene solution of BN-2Cz (0.01 mM) and DTNA (Figure 3a), accompanied by a significantly prolonged fluorescence lifetimes (τ_{DF} = 287 μs for BN-2Cz/1,4-DTNA system, 134 μs for BN-2Cz/1,5-DTNA system), clearly manifesting the long-lived triplet-mediated mechanism (Supporting Information Figure S23a).[19] Likewise, strong delayed fluorescence in the UV region could also be obtained by using BN-2Cz-*t*Bu (Figure 3a and Supporting Information Figure S23b). In all these systems, remarkable anti-Stokes shifts ranging from 0.91 eV (375 ← 517 nm) for 1,4-DTNA as acceptor to 0.98 eV (367 ← 517 nm) for 1,5-DTNA as acceptor were recorded, deduced by the energy difference between excitation wavelengths and the maximum UC emission peaks. Of particular note, since the red-shifted absorption band of BN-2Cz-*t*Bu extended down to over 540 nm, photoexcitation of the BN-2Cz-*t*Bu/1,5-DTNA system with a 532 nm laser was also feasible to produce intense UC emission (Supporting Information Figure S29c), offering a remarkable anti-Stokes shift up to 1.05 eV (367 ← 532 nm). To the best of our knowledge, this is the first research reported to realize efficient low-power green-to-UV TTA-UC, with unprecedented anti-Stokes shift

DOI: 10.31635/ccschem.022.202101507
Citation: *CCS Chem.* **2022**, 4, 3852–3863
Link to VoR: https://doi.org/10.31635/ccschem.022.202101507

values for visible-to-UV upconversion systems (Supporting Information Table S1 and Scheme 1c).

The upconversion quantum yield values (Φ_{UC}', with the theoretical limit standardized to be 100%, Supporting Information Table S7) deduced by the relative quantum yield method of BN-2Cz (0.01 mM) were up to 8.6% and 6.9% when pairing with 1,4-DTNA and 1,5-DTNA, respectively, under 517 nm excitation (Supporting Information Figures S28 and S29a). The higher values acquired by using 1,4-DTNA were in line with the acceptor's superior absolute fluorescence quantum yield. Switching the sensitizer to BN-2Cz-*t*Bu (0.01 mM) led to decreased Φ_{UC}'s (3.7% for 1,4-DTNA as acceptor, 3.4% for 1,5-DTNA as acceptor), largely ascribed to the inferior ISC rate and TTET efficiencies. Because of the low concentration of BN-2Cz-*t*Bu, the effect of exothermic RTET was considered to be marginal here, as proved by only the faint long-lived delayed component induced by RTET (DF') of BN-2Cz-*t*Bu (τ_{DF}' = 144 μs, Supporting Information Figure S21, see Supporting Information for detailed discussion). To our great delight, the Φ_{UC}' values of BN-2Cz-*t*Bu-based systems under 532 nm excitation could still approach 4.4% with 1,4-DTNA as acceptor and 2.7% with 1,5-DTNA (Supporting Information Figure S29c and Table S7). These results are among the best records for purely organic visible-to-UV upconversion systems (Scheme 1c and Supporting Information Table S1). It is envisaged that the efficiencies could be further promoted by structural optimization of the MR-TADF sensitizer to enhance the Φ_{ISC} (i.e., introducing heavy elements such as Ge, S, Se).

The threshold excitation power density I_{th}, where a quadratic-to-linear dependence of upconversion intensity on excitation power densities occurs, is another key indicator to evaluate TTA-UC systems besides conversion wavelengths and efficiencies.[51–53] According to the equation $I_{th} = 2(k_0^T)^2/(\gamma_{TT}\alpha\phi_{TTET})$, where the k_0^T is the triplet state decay rate of the acceptor, γ_{TT} is the second-order decay rate for TTA, and α is the extinction coefficient of the sensitizer, this parameter directly associates with the absorbance of sensitizer and Φ_{TTET}.[54] Therefore, increasing the concentration of sensitizer would usually lead to smaller I_{th} value for the same TTA-UC system. As illustrated in Figure 3b, the BN-2Cz/1,4-DTNA system showed a slope change from 2 to 1 in the log–log plot of UC emission against the laser power density, and the I_{th} was decreased from 209 mW cm^{-2} (Supporting Information Figures S24 and S26) to 15.8 mW cm^{-2} by increasing the concentration of BN-2Cz from 0.01 to 0.1 mM. Due to a larger molar extinction coefficient of BN-2Cz-*t*Bu at 517 nm, I_{th} was further reduced to 9.2 mW cm^{-2} in BN-2Cz-*t*Bu (0.1 mM)/1,4-DTNA, a value 88% lower than that of the reported vis-to-UV TTA-UC system adopting conventional TADF sensitizer (75 mW cm^{-2}).[55] According to Figure 3c, the Φ_{UC}' values were maintained as high as 7.5% for these samples even with increased concentration of sensitizer (0.1 mM), indicating that the undesirable photon reabsorption and singlet Förster energy transfer is probably not significant. This was also supported by only a slight decrease of acceptor's fluorescence emission intensity in the presence of 0.1 mM sensitizer (λ_{ex} = 330 nm, Supporting Information Figure S22). Remarkably, since the obtained I_{th}s were quite close to the solar irradiance (AM 1.5) of 2.6 mW cm^{-2} for BN-2Cz and 3.3 mW cm^{-2} for BN-2Cz-*t*Bu (0.1 mM, path length = 1 mm, Supporting Information Figure S27), the Φ_{UC}' values could still reach 1.3% at the solar irradiance. For 1,5-DTNA as acceptor, the I_{th} values were moderately raised to 41.8 mW cm^{-2} for BN-2Cz and 29.2 mW cm^{-2} for BN-2Cz-*t*Bu (Supporting Information Figure S25).

As an important aspect for practical applications, the inherent photostability of the upconversion systems was tested by monitoring the emission intensity at 370 nm under 517 nm photoexcitation with a power density of 160 mW cm^{-2}. After 1 h irradiation, the upconversion intensity of most systems remained above 90% of their initial value, that is, 94% for BN-2Cz/1,4-DTNA, 92% for BN-2Cz/1,5-DTNA (Figure 3d), and 90% for BN-2Cz-*t*Bu/1,4-DTNA (Supporting Information Figure S30). Comparatively, a 24% decay of intensity occurred in the BN-2Cz-*t*Bu/1,5-DTNA mixture, ascribable to the long-lived triplet excited state of BN-2Cz-*t*Bu and the lower TTET efficiency that may be susceptible to undesirable side reactions. These results reflect that high Φ_{TTET} may be beneficial to photostability.

Application of green-to-UV TTA-UC in photochemical transformations

Stimulated by the high upconversion efficiency, low threshold excitation intensity, and a large anti-Stokes shift of our green-to-UV upconversion systems, photochemical reactions using green light were subsequently demonstrated. Albeit near-infrared to visible/visible to visible TTA-UC has been applied to drive several organic reactions,[6,56] the majority of valuable photochemical transformations rely on UV irradiation due to insufficient energy input from a single visible photon.[57–59] These reactions are typically driven by mercury lamps at maximum 0.01–0.1 mM concentrations due to the attenuation of the excitation UV light being so strong that a uniform irradiation of the flask in combination with reasonable reaction times is impossible. Introducing the TTA-UC system to photochemical reactions could thus allow a nonvariable excitation light with minimum attenuation and basically allow unlimited high concentrations of the substrate. Meanwhile, existing reports about visible-to-UV TTA-UC for photochemical reaction all use intense blue light as the excitation source, which undoubtedly limits the application scope. Shifting the excitation wavelength to green light is desirable in terms of biocompatibility, penetration depth, and solar energy utilization efficiency since green light accounts for the highest proportion (AM 1.5) of sunlight.

DOI: 10.31635/ccschem.022.202101507
Citation: *CCS Chem.* **2022**, 4, 3852–3863
Link to VoR: https://doi.org/10.31635/ccschem.022.202101507

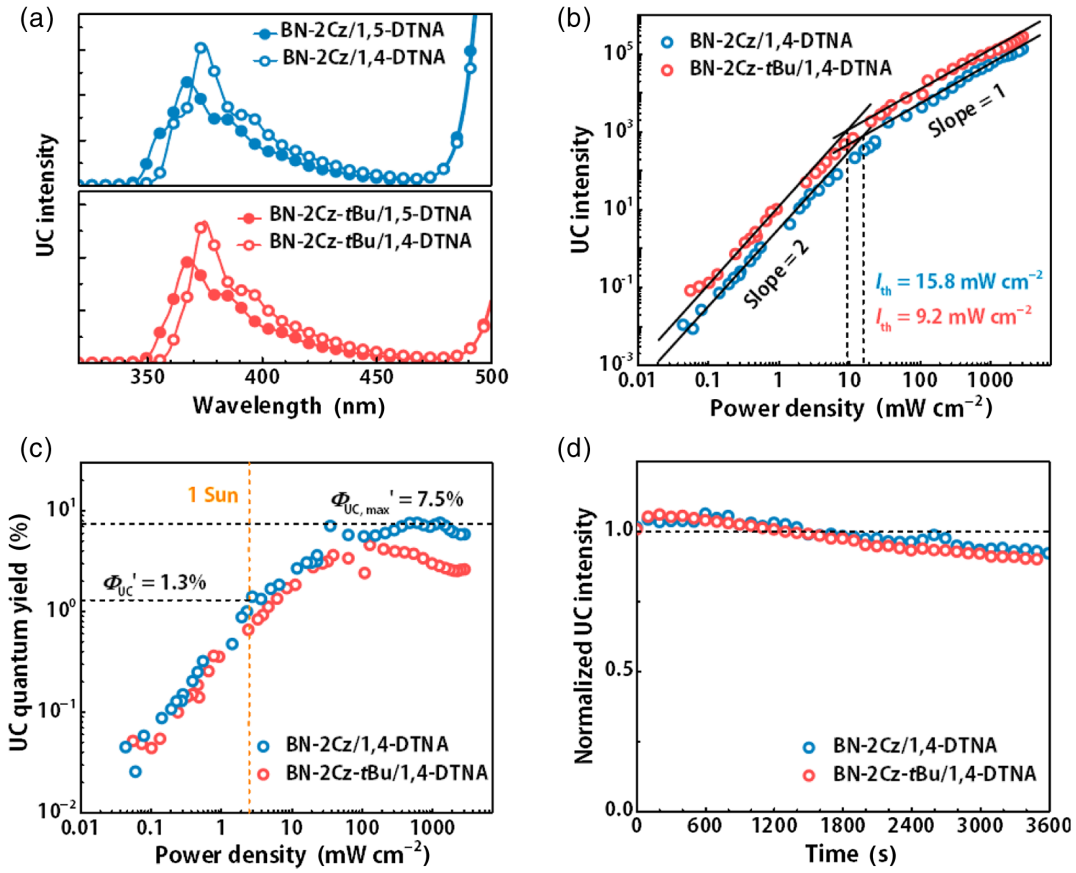

Figure 3 | *(a) Upconverted fluorescence emission spectra of sensitizers and acceptors, c[sensitizer] = 0.01 mM. (b) Double logarithmic plot of the upconverted fluorescence intensity as a function of excitation power density. (c) Double logarithmic plot of Φ_{UC}' as a function of excitation power density, red line indicates the intensity of sunlight (2.6 mW cm^{-2} for BN-2Cz, Supporting Information Figure S27). (d) Photostability studies by plotting normalized upconversion intensity at 370 nm under continuous irradiation with a 517 nm laser at I_{ex} = 160 mW cm^{-2}. Toluene as the solvent, c[sensitizer] = 0.1 mM.*

Photoactivated free radical polymerization has been a powerful synthetic tool applicable in dental care, nontoxic packaging, and 3D-printing due to its versatility and biocompatibility.[60-62] While typical photoinitiators only absorb short-wavelength photons (mostly UV), UV light sources are eco-unfriendly due to their formation of ozones and also present severe thermal effects and shallow penetration depth.[63] As a proof of concept, we integrated BN-2Cz/1,4-DTNA with the commercially available UV-absorbing 2,2-dimethoxy-2-phenylacetophenone (DMPA) as a green-light photoinitiating system, which was applied for the polymerization of *n*-butylacrylate (*n*BuA, as monomer) and ethylene dimethacrylate (EGDMA, as cross-linker).[57] The absorption band of DMPA overlapped with the TTA-UC emission greatly (Supporting Information Figure S31), and underwent the Norrish type I α-cleavage to produce free-radical species upon photon absorption. In a 2-mL-scale reaction, the mixture was rapidly transformed into a transparent freestanding gel featuring a storage modulus (G') of 3.7 × 10^4 Pa at 10 rad s^{-1} upon irradiation with a 517 nm laser (80 mW cm^{-2}, 2 min). Meanwhile no gelation occurred in control experiments in the absence of 1,4-DNTA after 30 min (Figure 4a and Supporting Information Figures S32, S33, and S37), confirming the necessity of TTA-UC. Benefiting from efficient UV photon production even under low excitation intensity, altering the light source to 512 nm LED (6.3 mW cm^{-2}, 20 min, Supporting Information Figures S34 and S35) yielded a gel at the same reaction scale. The increased penetrability of green light through the reaction media also enabled photocuring in a scale-up reaction (35 mL, curing depth = 4.5 cm) to produce homogeneous gel upon green LED exposure for 2 h (Supporting Information Figure S36). The above demonstrations clearly manifest the good sensitivity of the TTA-UC pair to weak incident light and its sufficient chemical stability to survive highly reactive radical species.

Instead of serving as internal lamps to trigger photoreactions, the TTA-UC pair could also be applied as an external UV source by segregating the upconversion

DOI: 10.31635/ccschem.022.202101507
Citation: *CCS Chem.* **2022**, 4, 3852–3863
Link to VoR: https://doi.org/10.31635/ccschem.022.202101507

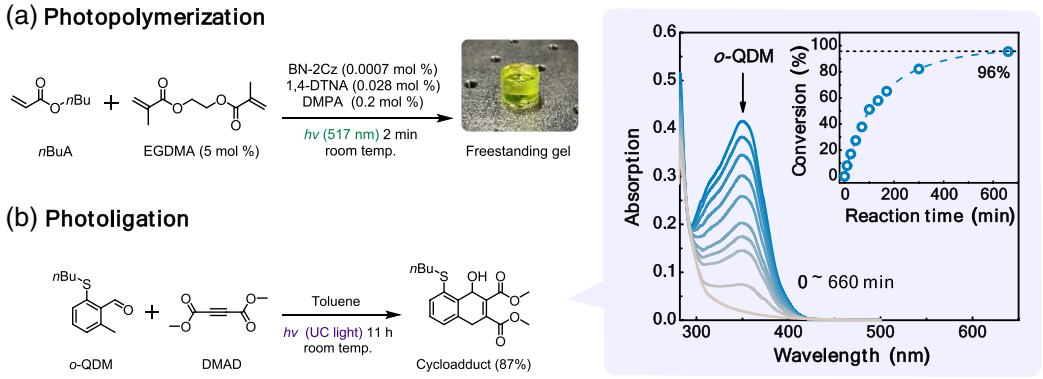

Figure 4 | *(a) Photoinitiated radical polymerization and digital photograph of the crosslinked gel product, λ_{ex} = 517 nm. (b) Photoligation reaction with upconverted light (left, see Supporting Information Figure S34 for experimental setup), together with absorption changes of the reaction mixture with increased photoirradiation time (right) and conversion of o-QDM reactant (right inset), c[o-QDM] = 5 mM, c[DMAD] = 6.25 mM. c[BN-2Cz] = 0.05 mM, c[1,4-DTNA] = 1 mM, λ_{ex} = 517 nm, toluene as the solvent.*

system and reaction system into two different vessels. This strategy is particularly useful under certain circumstances such as thermodynamically challenging photoreactions and may also avoid unwanted absorption/emission interference in product detection, simplify the workup procedure in photo-isomerization, or photo-click reactions.[64] To establish this concept, the UV-induced ligation of *o*-quinodimethanes, a noncatalyzed Diels-Alder reaction recently reported by Goldmann et al.[58] (Figure 4b), was selected as the model reaction. As most of the noncatalyzed photoligations are operable only by UV irradiation, it is hence of great significance to extend the excitation to the long-wavelength region by leveraging TTA-UC. Specifically, by immersing the inner vial containing BN-2Cz/1,4-DTNA in the solution mixture of two substrates *o*-methylbenzaldehydes (*o*-QDM, photocaged diene) and dimethyl acetylenedicarboxylate (DMAD, dienophile) (Supporting Information Figure S38), an efficient reaction took place when excited with a 517 nm laser beam (1500 mW cm^{-2}). As shown in Figure 4b, the n–π^* band absorption intensity of *o*-QDM at 350 nm (Supporting Information Figure S39) gradually decreased with increasing photoirradiation time, clearly suggesting the depletion of *o*-QDM.[58] The conversion of *o*-QDM reached 96% after photoirradiation of 11 h (Figure 4b inset) to provide the Diels-Alder adduct and the 4π-electrocyclization side product in a similar ratio (90:10) with the preceding result based on ^{1}H NMR measurement.[58] The turnover number for the reaction mixture was 240 regarding the sensitizer. Comparatively, less than 5% *o*-QDM was converted in the absence of the inner vial (control) due to energy mismatch between the excitation wavelength (517 nm) and absorption of *o*-QDM (<420 nm) (Supporting Information Figure S41), indicating the photoligation was enabled via reabsorption of TTA-UC emission by the substrate (Supporting Information Figure S40). In addition, under green LED (6.3 mW cm^{-2}) irradiance, a moderate conversion of *o*-QDM (11%) was still noticed with 18 h photoirradiation, while negligible conversion (<1%) took place in the control experiment (Supporting Information Figure S42). The long-term stability and high efficiency reflected herein holds promise for the use of these TTA-UC pairs in other challenging photochemical transformations under mild visible-light excitation.

Conclusion

To sum up, a series of pure organic MR-TADF sensitizers featuring unique electronic structures have been developed and applied to construct green-to-UV TTA-UC systems with energetically suitable acceptors. Due to small VR and the tiny ΔE_{ST} of the MR-TADF compounds, the energy loss is minimized during the triplet sensitization process, eventually leading to unprecedented energy gain, up to 1.05 eV in the visible-to-UV region. In addition, benefiting from the large molar extinction coefficient, high ISC yield, and long triplet lifetime of the sensitizers, the TTA-UC system exhibited high Φ_{UC}' (~7.5%) with low I_{th} values (~15.8 mW cm^{-2}), close to solar irradiance. The TTA-UC pairs can be utilized as stable internal or external phototransducers to activate UV-dependent polymerization and catalyst-free ligation under green light irradiation with weak intensity. Considering the structural versatility of MR-TADF compounds, there is still plenty of room to improve the comprehensive performance of visible-to-UV molecular upconverters, which would great promise for a variety of practical applications, including photovoltaics and photocatalysis.

DOI: 10.31635/ccschem.022.202101507
Citation: *CCS Chem.* **2022**, 4, 3852–3863
Link to VoR: https://doi.org/10.31635/ccschem.022.202101507

Supporting Information

Supporting Information is available and includes experimental instruments and measurement processes; a summary of reported visible-to-UV TTA-UC; synthesis and characterization of triplet sensitizers and acceptors; transient PL spectra of sensitizers; DFT and TD-DFT calculations results; a TTET study; TTA-UC spectra; TTA-UC quantum yields and photostability; and photopolymerization and photoligation with TTA-UC.

Conflict of Interest

There is no conflict of interest to report.

Funding Information

This research was made possible as a result of several generous grants from the National Natural Science Foundation of China (grant nos. 51903159 and 91833304) and the Shenzhen Science and Technology Program (grant nos. KQTD20170330110107046 and JCYJ20190808151209557).

Preprint Statement

Research presented in this article was posted on a preprint server prior to publication in *CCS Chemistry*. The corresponding preprint article can be found here: 10.33774/chemrxiv-2021-mq00r-v2; https://chemrxiv.org/engage/chemrxiv/article-details/60dd5eb5e9241988cce15ed5

Acknowledgments

We thank the Instrumental Analysis Center of Shenzhen University for analytical support. The authors also thank Prof. Zhichao Yan from Shenzhen University for rheology measurement.

References

1. Gray, V.; Dzebo, D.; Abrahamsson, M.; Albinsson, B.; Moth-Poulsen, K. Triplet-Triplet Annihilation Photon-Upconversion: Towards Solar Energy Applications. *Phys. Chem. Chem. Phys.* **2014**, *16*, 10345–10352.
2. Zhao, J.; Ji, S.; Guo, H. Triplet–Triplet Annihilation Based Upconversion: From Triplet Sensitizers and Triplet Acceptors to Upconversion Quantum Yields. *RSC Adv.* **2011**, *1*, 937–950.
3. Joarder, B.; Yanai, N.; Kimizuka, N. Solid-State Photon Upconversion Materials: Structural Integrity and Triplet-Singlet Dual Energy Migration. *J. Phys. Chem. Lett.* **2018**, *9*, 4613–4624.
4. Cheng, Y. Y.; Fückel, B.; MacQueen, R. W.; Khoury, T.; Clady, R. G. C. R.; Schulze, T. F.; Ekins-Daukes, N. J.; Crossley, M. J.; Stannowski, B.; Lips, K.; Schmidt, T. W. Improving the Light-Harvesting of Amorphous Silicon Solar Cells with Photochemical Upconversion. *Energy Environ. Sci.* **2012**, *5*, 6953–6959.
5. Hill, S. P.; Hanson, K. Harnessing Molecular Photon Upconversion in a Solar Cell at Sub-Solar Irradiance: Role of the Redox Mediator. *J. Am. Chem. Soc.* **2017**, *139*, 10988–10991.
6. Bilger, J. B.; Kerzig, C.; Larsen, C. B.; Wenger, O. S. A Photorobust Mo(0) Complex Mimicking $[Os(2,2\text{-Bipyridine})_3]^{2+}$ and Its Application in Red-to-Blue Upconversion. *J. Am. Chem. Soc.* **2021**, *143*, 1651–1663.
7. Pfund, B.; Steffen, D. M.; Schreier, M. R.; Bertrams, M. S.; Ye, C.; Borjesson, K.; Wenger, O. S.; Kerzig, C. UV Light Generation and Challenging Photoreactions Enabled by Upconversion in Water. *J. Am. Chem. Soc.* **2020**, *142*, 10468–10476.
8. Haring, M.; Perez-Ruiz, R.; Jacobi von Wangelin, A.; Diaz, D. D. Intragel Photoreduction of Aryl Halides by Green-to-Blue Upconversion under Aerobic Conditions. *Chem. Commun.* **2015**, *51*, 16848–16851.
9. Kimizuka, N.; Sasaki, Y.; Oshikawa, M.; Bharmoria, P.; Kouno, H.; Hayashi-Takagi, A.; Sato, M.; Ajioka, I.; Yanai, N. Near-Infrared Optogenetic Genome Engineering Based on Photon Upconversion Hydrogels. *Angew. Chem. Int. Ed.* **2019**, *58*, 17827–17833.
10. Yang, Z.-S.; Ning, Y.; Yin, H.-Y.; Zhang, J.-L. Lutetium(III) Porphyrinoids as Effective Triplet Photosensitizers for Photon Upconversion Based on Triplet–Triplet Annihilation. *Inorg. Chem. Front.* **2018**, *5*, 2291–2299.
11. Graf von Reventlow, L.; Bremer, M.; Ebenhoch, B.; Gerken, M.; Schmidt, T. W.; Colsmann, A. An Add-On Organic Green-to-Blue Photon-Upconversion Layer for Organic Light Emitting Diodes. *J. Mater. Chem. C* **2018**, *6*, 3845–3848.
12. Han, J.; Duan, P.; Li, X.; Liu, M. H. Amplification of Circularly Polarized Luminescence through Triplet-Triplet Annihilation-Based Photon Upconversion. *J. Am. Chem. Soc.* **2017**, *139*, 9783–9786.
13. Huang, L., Zhao, Y., Zhang, H., Huang, K., Yang, J., Han, G. Expanding Anti-Stokes Shifting in Triplet-Triplet Annihilation Upconversion for in Vivo Anticancer Prodrug Activation. *Angew. Chem. Int. Ed.* **2017**, *56*, 14400–14404.
14. Wei, Y.; Zheng, M.; Chen, L.; Zhou, X.; Liu, S. Near-Infrared to Violet Triplet-Triplet Annihilation Fluorescence Upconversion of Os(II) Complexes by Strong Spin-Forbidden Transition. *Dalton Trans.* **2019**, *48*, 11763–11771.
15. Haruki, R.; Sasaki, Y.; Masutani, K.; Yanai, N.; Kimizuka, N. Leaping across the Visible Range: Near-Infrared-to-Violet Photon Upconversion Employing a Silyl-Substituted Anthracene. *Chem. Commun.* **2020**, *56*, 7017–7020.
16. Majek, M.; Faltermeier, U.; Dick, B.; Perez-Ruiz, R.; Jacobi von Wangelin, A. Application of Visible-to-UV Photon Upconversion to Photoredox Catalysis: The Activation of Aryl Bromides. *Chem. Eur. J.* **2015**, *21*, 15496–15501.

DOI: 10.31635/ccschem.022.202101507
Citation: *CCS Chem.* **2022**, 4, 3852–3863
Link to VoR: https://doi.org/10.31635/ccschem.022.202101507

17. Khnayzer, R. S.; Blumhoff, J.; Harrington, J. A.; Haefele, A.; Deng, F.; Castellano, F. N. Upconversion-Powered Photoelectrochemistry. *Chem. Commun.* **2012**, *48*, 209–211.
18. Takata, T.; Jiang, J.; Sakata, Y.; Nakabayashi, M.; Shibata, N.; Nandal, V.; Seki, K.; Hisatomi, T.; Domen, K. Photocatalytic Water Splitting with a Quantum Efficiency of Almost Unity. *Nature* **2020**, *581*, 411–414.
19. Harada, N.; Sasaki, Y.; Hosoyamada, M.; Kimizuka, N.; Yanai, N. Discovery of Key TIPS-Naphthalene for Efficient Visible-to-UV Photon Upconversion under Sunlight and Room Light. *Angew. Chem. Int. Ed.* **2020**, *133*, 144–149.
20. Yanai, N.; Kozue, M.; Amemori, S.; Kabe, R.; Adachi, C.; Kimizuka, N. Increased Vis-to-UV Upconversion Performance by Energy Level Matching between a TADF Donor and High Triplet Energy Acceptors. *J. Mater. Chem. C* **2016**, *4*, 6447–6451.
21. Duan, P.; Yanai, N.; Kimizuka, N. A Bis-Cyclometalated Iridium Complex as a Benchmark Sensitizer for Efficient Visible-to-UV Photon Upconversion. *Chem. Commun.* **2014**, *50*, 13111–13113.
22. Han, J.; Jiang, Y.; Obolda, A.; Duan, P.; Li, F.; Liu, M. Doublet–Triplet Energy Transfer-Dominated Photon Upconversion. *J. Phys. Chem. Lett.* **2017**, *8*, 5865–5870.
23. Wei, Y.; Xian, H.; Lv, X.; Ni, F.; Cao, X.; Yang, C. Triplet–Triplet Annihilation Upconversion with Reversible Emission-Tunability Induced by Chemical-Stimuli: A Remote Modulator for Photocontrol Isomerization. *Mater. Horizons* **2021**, *8*, 606–611.
24. Wei, Y.; Li, Y.; Zheng, M.; Zhou, X.; Zou, Y.; Yang, C. Simultaneously High Upconversion Efficiency and Large Anti-Stokes Shift by Using Os(II) Complex Dyad as Triplet Photosensitizer. *Adv. Opt. Mater.* **2020**, *8*, 1902157.
25. Amemori, S.; Sasaki, Y.; Yanai, N.; Kimizuka, N. Near-Infrared-to-Visible Photon Upconversion Sensitized by a Metal Complex with Spin-Forbidden yet Strong S_0-T_1 Absorption. *J. Am. Chem. Soc.* **2016**, *138*, 8702–8705.
26. Qi, Y.; Ning, W.; Zou, Y.; Cao, X.; Gong, S.; Yang, C. Peripheral Decoration of Multi-Resonance Molecules as a Versatile Approach for Simultaneous Long-Wavelength and Narrowband Emission. *Adv. Funct. Mater.* **2021**, *31*, 2102017.
27. Peng, J.; Guo, X.; Jiang, X.; Zhao, D.; Ma, Y. Developing Efficient Heavy-Atom-Free Photosensitizers Applicable to TTA Upconversion in Polymer Films. *Chem. Sci.* **2016**, *7*, 1233–1237.
28. Jiang, X.; Guo, X.; Peng, J.; Zhao, D.; Ma, Y. Triplet-Triplet Annihilation Photon Upconversion in Polymer Thin Film: Sensitizer Design. *ACS Appl. Mater. Interfaces* **2016**, *8*, 11441–11449.
29. Lee, H.-L.; Lee, M.-S.; Park, H.; Han, W.-S.; Kim, J.-H. Visible-to-UV Triplet-Triplet Annihilation Upconversion from a Thermally Activated Delayed Fluorescence/Pyrene Pair in an Air-Saturated Solution. *Korean J. Chem. Eng.* **2019**, *36*, 1791–1798.
30. Singhrachford, T. N.; Castellano, F. N. Low Power Visible-to-UV Upconversion. *J. Phys. Chem. A* **2009**, *113*, 5912–5917.
31. Murakami, Y.; Motooka, A.; Enomoto, R.; Niimi, K.; Kaiho, A.; Kiyoyanagi, N. Visible-to-Ultraviolet (<340 nm) Photon Upconversion by Triplet-Triplet Annihilation in Solvents. *Phys. Chem. Chem. Phys.* **2020**, *22*, 27134–27143.
32. Gray, V.; Xia, P.; Huang, Z.; Moses, E.; Fast, A.; Fishman, D. A.; Vullev, V. I.; Abrahamsson, M.; Moth-Poulsen, K.; Lee Tang, M. Cds/Zns Core-Shell Nanocrystal Photosensitizers for Visible to UV Upconversion. *Chem. Sci.* **2017**, *8*, 5488–5496.
33. Okumura, K.; Yanai, N.; Kimizuka, N. Visible-to-UV Photon Upconversion Sensitized by Lead Halide Perovskite Nanocrystals. *Chem. Lett.* **2019**, *48*, 1347–1350.
34. He, S.; Luo, X.; Liu, X.; Li, Y.; Wu, K. Visible-to-Ultraviolet Upconversion Efficiency above 10% Sensitized by Quantum-Confined Perovskite Nanocrystals. *J. Phys. Chem. Lett.* **2019**, *10*, 5036–5040.
35. Hou, L.; Olesund, A.; Thurakkal, S.; Zhang, X.; Albinsson, B. Efficient Visible-to-UV Photon Upconversion Systems Based on CdS Nanocrystals Modified with Triplet Energy Mediators. *Adv. Funct. Mater.* **2021**, *31*, 2106198.
36. Wei, Y.; Zhou, M.; Zhou, Q.; Zhou, X.; Liu, S.; Zhang, S.; Zhang, B. Triplet-Triplet Annihilation Upconversion Kinetics of C_{60}-Bodipy Dyads as Organic Triplet Photosensitizers. *Phys. Chem. Chem. Phys.* **2017**, *19*, 22049–22060.
37. Wang, Z.; Zhao, J.; Barbon, A.; Toffoletti, A.; Liu, Y.; An, Y.; Xu, L.; Karatay, A.; Yaglioglu, H. G.; Yildiz, E. A. Radical Enhanced Intersystem Crossing in New Bodipy Derivatives and Application for Efficient Triplet-Triplet Annihilation Upconversion. *J. Am. Chem. Soc.* **2017**, *139*, 7831–7842.
38. Hatakeyama, T.; Shiren, K.; Nakajima, K.; Nomura, S.; Nakatsuka, S.; Kinoshita, K.; Ni, J.; Ono, Y.; Ikuta, T. Ultrapure Blue Thermally Activated Delayed Fluorescence Molecules: Efficient HOMO-LUMO Separation by the Multiple Resonance Effect. *Adv. Mater.* **2016**, *28*, 2777–2781.
39. Oda, S.; Kumano, W.; Hama, T.; Kawasumi, R.; Yoshiura, K.; Hatakeyama, T. Carbazole-Based Dabna Analogues as Highly Efficient Thermally Activated Delayed Fluorescence Materials for Narrowband Organic Light-Emitting Diodes. *Angew. Chem. Int. Ed.* **2021**, *60*, 2882–2886.
40. Zhang, Y.; Zhang, D.; Wei, J.; Liu, Z.; Lu, Y.; Duan, L. Multi-Resonance Induced Thermally Activated Delayed Fluorophores for Narrowband Green OLEDs. *Angew. Chem. Int. Ed.* **2019**, *58*, 16912–16917.
41. Kondo, Y.; Yoshiura, K.; Kitera, S.; Nishi, H.; Oda, S.; Gotoh, H.; Sasada, Y.; Yanai, M.; Hatakeyama, T. Narrowband Deep-Blue Organic Light-Emitting Diode Featuring an Organoboron-Based Emitter. *Nat. Photonics* **2019**, *13*, 678–682.
42. Yang, M.; Park, I. S.; Yasuda, T. Full-Color, Narrowband, and High-Efficiency Electroluminescence from Boron and Carbazole Embedded Polycyclic Heteroaromatics. *J. Am. Chem. Soc.* **2020**, *142*, 19468–19472.
43. Xu, Y.; Wang, Q.; Cai, X.; Li, C.; Wang, Y. Highly Efficient Electroluminescence from Narrowband Green Circularly Polarized Multiple Resonance Thermally Activated Delayed Fluorescence Enantiomers. *Adv. Mater.* **2021**, *33*, 2100652.
44. Stavrou, K.; Danos, A.; Hama, T.; Hatakeyama, T.; Monkman, A. Hot Vibrational States in a High-Performance Multiple Resonance Emitter and the Effect of Excimer

DOI: 10.31635/ccschem.022.202101507
Citation: *CCS Chem.* **2022**, 4, 3852–3863
Link to VoR: https://doi.org/10.31635/ccschem.022.202101507

Quenching on Organic Light-Emitting Diodes. *ACS Appl. Mater. Interfaces* **2021**, *13*, 8643–8655.
45. Tanaka, H.; Oda, S.; Ricci, G.; Gotoh, H.; Tabata, K.; Kawasumi, R.; Beljonne, D.; Olivier, Y.; Hatakeyama, T. Hypsochromic Shift of Multiple-Resonance-Induced Thermally Activated Delayed Fluorescence by Oxygen Atom Incorporation. *Angew. Chem. Int. Ed.* **2021**, *60*, 17910–17914.
46. Zhao, J.; Chen, K.; Hou, Y.; Che, Y.; Liu, L.; Jia, D. Recent Progress in Heavy Atom-Free Organic Compounds Showing Unexpected Intersystem Crossing (ISC) Ability. *Org. Biomol. Chem.* **2018**, *16*, 3692–3701.
47. Wu, K.; Zhang, T.; Wang, Z.; Wang, L.; Zhan, L.; Gong, S.; Zhong, C.; Lu, Z.-H.; Zhang, S.; Yang, C. De Novo Design of Excited-State Intramolecular Proton Transfer Emitters Via a Thermally Activated Delayed Fluorescence Channel. *J. Am. Chem. Soc.* **2018**, *140*, 8877–8886.
48. Li, L.; Zeng, Y.; Chen, J.; Yu, T.; Hu, R.; Yang, G.; Li, Y. Thermally Activated Delayed Fluorescence via Triplet Fusion. *J. Phys. Chem. Lett.* **2019**, *10*, 6239–6245.
49. Wei, Y.; Wang, Y.; Zhou, Q.; Zhang, S.; Zhang, B.; Zhou, X.; Liu, S. Solvent Effects on Triplet–Triplet Annihilation Upconversion Kinetics of Perylene with a Bodipy-Phenyl-C_{60} Photosensitizer. *Phys. Chem. Chem. Phys.* **2020**, *22*, 26372–26382.
50. Sandros, K. Transfer of Triplet State Energy in Fluid Solutions. III. Reversible Energy Transfer. *Acta Chem. Scand.* **1964**, *18*, 2355–2374.
51. Monguzzi, A.; Mezyk, J.; Scotognella, F.; Tubino, R.; Meinardi, F. Upconversion-Induced Fluorescence in Multicomponent Systems: Steady-State Excitation Power Threshold. *Phys. Rev. B* **2008**, *78*, 195112.
52. Cheng, Y. Y.; Fückel, B.; Khoury, T.; Clady, R. G.; Tayebjee, M. J.; Ekins-Daukes, N.; Crossley, M. J.; Schmidt, T. W. Kinetic Analysis of Photochemical Upconversion by Triplet–Triplet Annihilation: Beyond Any Spin Statistical Limit. *J. Phys. Chem. Lett.* **2010**, *1*, 1795–1799.
53. Haefele, A.; Blumhoff, J.; Khnayzer, R. S.; Castellano, F. N. Getting to the (Square) Root of the Problem: How to Make Noncoherent Pumped Upconversion Linear. *J. Phys. Chem. Lett.* **2012**, *3*, 299–303.
54. Monguzzi, A.; Tubino, R.; Hoseinkhani, S.; Campione, M.; Meinardi, F. Low Power, Non-Coherent Sensitized Photon Up-Conversion: Modelling and Perspectives. *Phys. Chem. Chem. Phys.* **2012**, *14*, 4322–4332.
55. Han, D.; Yang, X.; Han, J.; Zhou, J.; Jiao, T.; Duan, P. Sequentially Amplified Circularly Polarized Ultraviolet Luminescence for Enantioselective Photopolymerization. *Nat. Commun.* **2020**, *11*, 5659.
56. Ravetz, B. D.; Pun, A. B.; Churchill, E. M.; Congreve, D. N.; Rovis, T.; Campos, L. M. Photoredox Catalysis Using Infrared Light via Triplet Fusion Upconversion. *Nature* **2019**, *565*, 343–346.
57. Croisant, M.; Bretz, S. L.; Konkolewicz, D. Investigating Radical Reactivity and Structure–Property Relationships through Photopolymerization. *J. Chem. Educ.* **2019**, *96*, 348–353.
58. Feist, F.; Rodrigues, L. L.; Walden, S. L.; Krappitz, T. W.; Dargaville, T. R.; Weil, T.; Goldmann, A. S.; Blinco, J. P.; Barner-Kowollik, C. Light-Induced Ligation of o-Quinodimethanes with Gated Fluorescence Self-Reporting. *J. Am. Chem. Soc.* **2020**, *142*, 7744–7748.
59. Alam, M. Z.; Shibahara, A.; Ogata, T.; Kurihara, S. Synthesis of Azobenzene-Functionalized Star Polymers via Raft and Their Photoresponsive Properties. *Polymer* **2011**, *52*, 3696–3703.
60. Xu, Y.; Li, C.; Li, Z.; Wang, Q.; Cai, X.; Wei, J.; Wang, Y. Constructing Charge-Transfer Excited States Based on Frontier Molecular Orbital Engineering: Narrowband Green Electroluminescence with High Color Purity and Efficiency. *Angew. Chem. Int. Ed.* **2020**, *59*, 17442–17446.
61. Corrigan, N.; Yeow, J.; Judzewitsch, P.; Xu, J.; Boyer, C. Seeing the Light: Advancing Materials Chemistry through Photopolymerization. *Angew. Chem. Int. Ed.* **2019**, *58*, 5170–5189.
62. Dietlin, C.; Schweizer, S.; Xiao, P.; Zhang, J.; Morlet-Savary, F.; Graff, B.; Fouassier, J.-P.; Lalevée, J. Photopolymerization Upon Leds: New Photoinitiating Systems and Strategies. *Polym. Chem.* **2015**, *6*, 3895–3912.
63. Bagheri, A.; Jin, J. Photopolymerization in 3D Printing. *ACS Appl. Polym. Mater.* **2019**, *1*, 593–611.
64. Tuten, B. T.; Wiedbrauk, S.; Barner-Kowollik, C. Contemporary Catalyst-Free Photochemistry in Synthetic Macromolecular Science. *Prog. Polym. Sci.* **2020**, *100*, 101183.

DOI: 10.31635/ccschem.022.202101507
Citation: *CCS Chem.* **2022**, 4, 3852–3863
Link to VoR: https://doi.org/10.31635/ccschem.022.202101507